



HAL
open science

Experimental study of flight effects on underexpanded supersonic jet noise

Benoît André, Thomas Castelain, Christophe Bailly

► **To cite this version:**

Benoît André, Thomas Castelain, Christophe Bailly. Experimental study of flight effects on underexpanded supersonic jet noise. Acoustics 2012, Apr 2012, Nantes, France. hal-00811019

HAL Id: hal-00811019

<https://hal.science/hal-00811019>

Submitted on 23 Apr 2012

HAL is a multi-disciplinary open access archive for the deposit and dissemination of scientific research documents, whether they are published or not. The documents may come from teaching and research institutions in France or abroad, or from public or private research centers.

L'archive ouverte pluridisciplinaire **HAL**, est destinée au dépôt et à la diffusion de documents scientifiques de niveau recherche, publiés ou non, émanant des établissements d'enseignement et de recherche français ou étrangers, des laboratoires publics ou privés.



ACOUSTICS 2012

Experimental study of flight effects on underexpanded supersonic jet noise

B. André^a, T. Castelain^{a,b} and C. Bailly^a

^aLaboratoire de Mécanique des Fluides et d'Acoustique, 36 Av Guy de Collongue 69134
Ecully Cedex

^bUniversité de Lyon, 43 Boulevard du 11 Novembre 1918, 69622 Villeurbanne Cedex, France
benoit.andre@ec-lyon.fr

An experimental study of flight effects on the broadband shock-associated noise (BBSAN) component of an under-expanded supersonic jet has been performed using a free jet facility. Far field acoustic measurements and particle image velocimetry (PIV) have been employed to characterise the flight effects both on the acoustic emission and on the aerodynamics of the jet. The BBSAN peak frequency decreases in flight when observed in the far field, both from a constant emission angle and a constant convected angle. Taking a constant convection velocity in flight allows a better agreement between the measurements and the peak frequency prediction formula by Tam (*Journal of Sound and Vibration*, 1991) to be obtained. A slight decrease of the BBSAN sound pressure level due to flight has been identified. PIV data show that the shock strength seems practically independent on the flight velocity while the turbulence levels considerably decrease in flight. It is possible that the flight-induced source extension compensates the lower turbulence levels to produce the somewhat unchanged levels of BBSAN observed.

1 Introduction

The largest part of the current commercial aircraft fleet is powered by turbofan engines, in which a hot jet is embedded in a cold secondary jet. At typical cruise condition, this secondary stream is supersonic and imperfectly expanded, which induces a shock-cell structure inside the jet plume. It has long been recognised that this was responsible for additional noise components beside the turbulent mixing noise also emitted by subsonic jets: the so-called shock-associated noise components. One of them, referred to as screech [1, 2], is tonal and associated with a self-excited feedback loop. Vortical disturbances travelling downstream interact with the quasi-periodic shock-cell structure, which generates noise. Upon propagating upstream and reaching the nozzle exit, the emitted acoustic waves induce new disturbances in the initial mixing layer, which closes the loop. The loop is resonant for the screech frequency and its harmonics. Another part of shock-associated noise is broadband in nature and thus called broadband shock-associated noise (BBSAN). It has first been identified by Martlew [3]. Harper-Bourne & Fisher [4] subsequently proposed a semi-empirical model, based on Powell's model for screech and using new turbulence measurements in the jet mixing layer. BBSAN was seen as the interference pattern of a phased array of acoustic sources located at the end of each shock cell. Their model was assessed through extensive acoustic measurements by Tanna [5]. An alternative model was later proposed by Tam & Tanna [6] which emphasized the coherent and non-localised character of the interaction between turbulent structures and shock-cell system. The BBSAN emission was regarded in that work as Mach wave radiation coming from the weak interaction between downstream travelling instability waves and the quasi-periodic shock-cell structure. However, the same formulae for peak frequency and BBSAN intensity were found as in Harper-Bourne & Fisher [4]. This theoretical framework was then further developed by Tam *et al.* [7, 8], which led to the prediction of near-field and far-field noise spectra.

In flight conditions, the shock-containing cold secondary jet is embedded in a subsonic outer flow arising from the aircraft motion. This prompted studies focusing on the flight effect on shock-associated noise. Bryce & Pinker [9] adapted Powell's [1] and Harper-Bourne & Fisher's [4] frequency formulae for screech and BBSAN to flight. Norum & Shearin [10, 11, 12] conducted detailed static pressure measurements to delineate the flight effects on the shock-cell structure, as well as extensive acoustic measurements, up to a flight Mach number of 0.4. This data was used by Tam [13] to evaluate the extension of his BBSAN model to flight conditions.

Broadband shock-associated noise has become an increasing concern for the aeronautical industry through the

use of composite materials, inducing lower sound transmission losses than classical metallic structures, in the next-generation aircraft fuselages. Recently, Viswanathan & Czech [14] studied flight effects on BBSAN by acoustic measurements. Rask *et al.* [15] utilized particle image velocimetry (PIV) along with pressure and acoustic measurements to characterise BBSAN from chevron nozzles in flight.

In the present contribution, flight effects on the frequency and amplitude of BBSAN are considered. The experimental set-up will first be presented in section 2. Then, flight effects on BBSAN will be characterised from acoustic measurements. Finally, PIV data will be presented and analysed against the acoustic results.

2 Experimental set-up

The same facility has been used for this work as already described in the study of flight effects on screech by the authors [16]. Only a brief account is given here. Flight is simulated in the present experiment by a free jet facility built in an anechoic environment. The supersonic jet, simulating the shock-containing cold secondary stream of a turbofan engine, is generated by a continuously operating compressor. It is unheated and exhausts through a 38.7 mm diameter axisymmetric contoured convergent nozzle. The secondary jet in the experiment, simulating the outer flow, comes from a fan system. It has a diameter of 200 mm and a maximal flight Mach number M_f of approximately 0.4. Both flows are coaxial and both nozzles have the same exit plane. The total pressure of the primary jet is recovered from a static pressure measurement performed about 15 primary nozzle diameters upstream of the exit. Total temperatures are also monitored in both jets. The adequacy of the primary-to-secondary nozzle diameter ratio to study shock-associated noise has been checked by means of a total pressure survey and is also clearly visible on the PIV results.

The PIV set-up consists of a Quantronix Darwin Duo Nd:YLF pulsed laser with two cavities, emitting coherent light of 527 nm wavelength in the form of pulses of 120 ns duration. The time delay between both pulses is 3 μ s. The light sheet width is about 1.7 mm and contains the median vertical plane of the primary jet. Olive oil seeding in the core jet is introduced 6 meters upstream of the exit by Laskin's nozzle generators. The particle diameter is estimated to be about 1 μ m. The secondary jet is also seeded by means of a smoke generator set at the air intake of the fan. Since the inner (supersonic) jet and its mixing layer with the secondary jet are of interest, no seeding of the ambient air was needed. The field of view is recorded by two identical high-speed CMOS Phantom cameras set side by side. The optical

assembly leads to a magnification factor of approximately 0.05 mm/pixel. The cameras and the laser light emission head, located at the end of an optical arm, are mounted on a frame allowing axial displacements. An axial extent of about 10 primary nozzle diameters has been investigated in a total of five axial stations for the PIV system. A new calibration has been performed at each new axial station. It has to be noted that the jet operating conditions had to be reset for each one of the five fields of view. For each axial location, 2000 independent image pairs have been recorded at 500 Hz. The image recording and processing have been performed using the Lavision Davis 7.0 software. The latter has been made by a multigrid iterative FFT-based cross-correlation technique down to windows of size 8×8 pixels² with 50% overlap. The final velocity fields have been filtered using Chauvenet's criterion, which is a statistical criterion aiming at objectively determining outliers.

Far-field acoustic spectra have been measured using 13 PCB Piezotronics 6.35 mm diameter microphones mounted on a polar antenna 2.02 m away from the primary nozzle exit. The microphones are located every 10° from 30 to 150° . In the following, the angles are measured from the downstream jet axis. The microphones being located outside of the secondary stream, angular and amplitude corrections have to be applied to the measured acoustic data to account for the refraction of the acoustic rays by the external shear layer. The corrections used in this work come from Amiet [17]. In particular, they relate different angles arising in the physical problem of interest, depicted in Fig. 1. The emission angle would be the angle of the acoustic rays in the absence of secondary flows. Because of the convection of the acoustic fronts, the rays propagate along the convected angle θ_c . θ is the refracted angle of the rays outgoing from the shear layer. The relation between θ_e and θ can be written using Snell's law of refraction. Furthermore, θ_e and θ_c are related by the velocity triangle depicted in the lower right corner in Fig. 1. Finally, the microphone angle θ_m is related to the others by the geometry of the problem, *i.e.* h and R_m . In the case of broadband shock-associated noise, the acoustic source has a finite spatial extent. Taking the centroid of the acoustic source to be located a particular number of shock-cell spacings downstream of the exit, the angle relations would be dependent on the jet fully expanded Mach number M_j . For simplicity, the acoustic source has here been considered to be located in the nozzle exit plane. Hence, a unique relation between all angles exist whatever the value of M_j . To summarise, the emission and convected angles corresponding to each microphone location change with M_f . Conversely, one cannot measure a spectrum at a particular value of θ_c or θ_e for any value of M_f , since the microphone positions are fixed. In order to complement the acoustic data obtained by the antenna while sticking to a chosen set of values for M_f , a single microphone has also been mounted on a rotating boom. So, fractional microphone angles could be reached and some plots could be completed.

3 Acoustics results

It is known that screech has a non-negligible influence on BBSAN [18]. Furthermore, flight-induced screech mode switching [16] can entail jumps in the peak frequency of BBSAN. Another disturbing effect of screech while studying

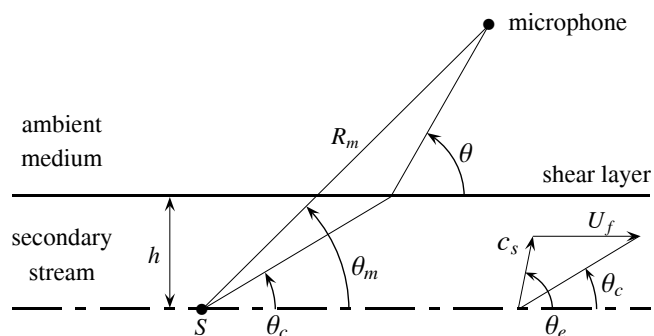


Figure 1: Definition of the geometry of the shear layer and of the angles of interest. h is the distance between the acoustic source S and the shear layer, R_m is the distance from acoustic source to the microphone. θ_e , θ_c , θ and θ_m are the emission, convected, refracted and microphone angles, respectively. The velocity triangle involves the speed of sound in the secondary stream c_s and the flight velocity, U_f .

BBSAN is the screech amplitude variation in flight, which was already identified by Norum & Shearin [10]. A very strong screech tends for instance to suppress BBSAN, as is clearly visible in Fig. 17 of [16]. In order to get rid of the questioning about the effect of screech, a notched nozzle has been used in the present experiment for its screech-suppressing capability [18]. However, screech tends to come back when the secondary flow is on, at high M_j . As a consequence, only the case of $M_j = 1.15$ will be discussed here, where screech was minimized and roughly homogeneous at all values of M_f .

Harper-Bourne & Fisher [4] and Tam & Tanna [6] found from quite different approaches the same formula for the peak frequency of BBSAN, f_p , in static conditions. It reads

$$f_p = \frac{U_c}{L(1 - M_c \cos \theta_m)} \quad (1)$$

where U_c is the convection velocity of vortical structures in the mixing layer, L is the shock spacing and M_c is the ratio of U_c and the speed of sound in the ambient medium. Bryce & Pinker [9] and Norum & Shearin [10] modified the peak frequency formula starting from the Harper-Bourne & Fisher's model to account for the presence of a secondary stream. In the latter reference, an angular correction is also developed. Tam [13] proposed as well a formula for f_p in flight using his instability wave theory. It has been checked that it gives practically the same estimations as the formula from Norum & Shearin [10] with angular correction. The formula by Tam [13] reads

$$f_p = \frac{U_c}{L \left\{ 1 + M_c \left[\frac{M_f (1 - M_f^2 \sin^2(\pi - \theta_c))^{1/2} + \cos(\pi - \theta_c)}{(1 - M_f^2)(1 - M_f^2 \sin^2(\pi - \theta_c))^{1/2}} \right] \right\}} \quad (2)$$

In the following, Eq. (2) is tested against measurements of the BBSAN peak frequency at θ_e and θ_c constant. To do so, the angular corrections from Amiet [17] are used to relate any chosen angle to the convected angle θ_c prior to the application of Eq. (2). A static shock-cell length of $1.03 \sqrt{M_j^2 - 1} D$, where D is the nozzle diameter of the supersonic jet, has been chosen, based on schlieren and static pressure measurements. The factor 1.03 has been obtained by averaging the downstream shock spacings, as suggested by Tam [8], the

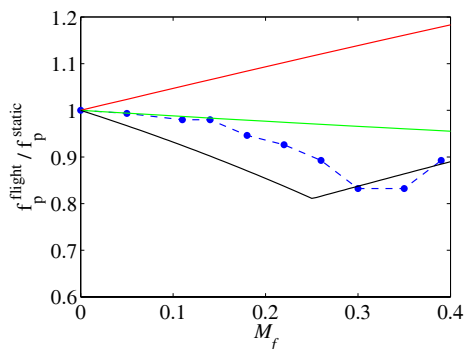


Figure 2: $f_p^{flight} / f_p^{static}$ for $M_j = 1.15$, $\theta_e = 80^\circ$.

• measurement points, — U_c from Eq. (3), — U_c from Eq. (4), — U_c from Murakami & Papamoschou [21].

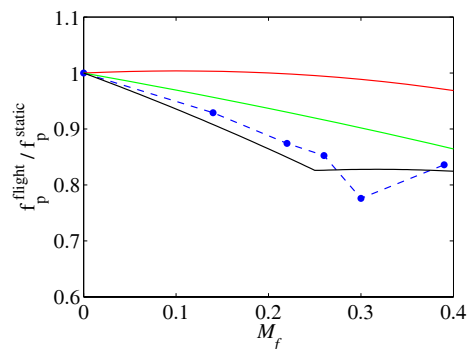


Figure 3: $f_p^{flight} / f_p^{static}$ for $M_j = 1.15$, $\theta_e = 130.5^\circ$.

• measurement points, — U_c from Eq. (3), — U_c from Eq. (4), — U_c from Murakami & Papamoschou [21].

first shock cells being weak sources of BBSAN [19]. Because of the thickness of the mixing layer existing several nozzle diameters downstream in the jet plume, the model of shock-cell length in flight developed by Morris [20] may not be accurate. A linear variation of shock spacing with M_f has been assumed here for simplicity, following Bryce & Pinker [9] and Tam [13]. The formula $L_{flight} = L_{static} (1 + 0.1 M_f)$ is in good agreement with experimental data by the authors and Norum & Shearin [12] around $M_j = 1.15$. It has to be noted that the factor 0.1 is much smaller than the value of 0.625 taken by Tam [13]. Three different expressions for U_c have been tested. The usual formulation [10, 13]

$$U_c = \alpha U_j + (1 - \alpha) U_f \quad (3)$$

where U_f is the flight velocity and U_j the fully expanded jet velocity, has been used with $\alpha = 0.65$ [18]. The second formulation is

$$U_c = \alpha U_j \quad (4)$$

as in [16]. Finally, an estimate of U_c developed by Murakami & Papamoschou [21] for coaxial supersonic jets has also been tried.

Absolute estimates have been found to be quite far off the experimental data, even at $M_f = 0$. The prediction formula tends to underestimate the BBSAN peak frequency, which was already noted, *e.g.* by Tanna [5]. Hence, only plots of $f_p^{flight} / f_p^{static}$ will be shown in the following. The evolution of this ratio against M_f is shown in Fig. 2 and 3 for constant emission angles θ_e of 80 and 130.5°, respectively. Considering the evolution of BBSAN for a constant θ_e allows the source modification due to flight to be isolated. Forward flight induces a slight increase in shock spacing L , inducing a reduced f_p . Depending on the expression taken for U_c , the effect of flight on f_p is contradictory. From Eq. (3), U_c increases with M_f , while it is independent on M_f by Eq. (4). In the model of Murakami & Papamoschou [21], U_c decreases with M_f . This explains the variation in the predictions of Fig. 2 and 3. The experimental points lie between the curves obtained using Eq. (4) and [21], while the predicted f_p increases using U_c from Eq. (3). The latter evolution is in agreement with the study by Norum & Shearin [10] but it contradicts the measured trend.

The evolution of $f_p^{flight} / f_p^{static}$ against M_f is shown in Fig. 4 and 5 for constant convected angles θ_c of 60 and 99.5°, respectively. Considering the evolution of BBSAN for a constant θ_c corresponds to the real situation of an observer located at a fixed position relatively to the jet, like an aircraft

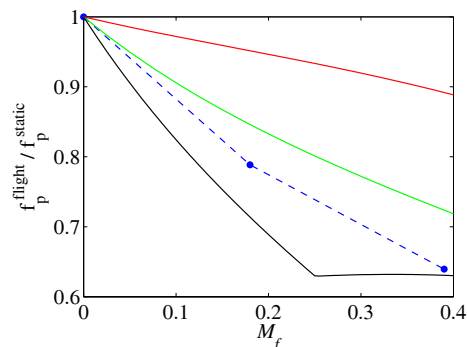


Figure 4: $f_p^{flight} / f_p^{static}$ for $M_j = 1.15$, $\theta_c = 60^\circ$.

• measurement points, — U_c from Eq. (3), — U_c from Eq. (4), — U_c from Murakami & Papamoschou [21].

passenger in the cabin. The same kind of figures are obtained as for a constant θ_e but the peak frequency decrease with M_f is more obvious. It is emphasized due to the convection, which bends downstream acoustic rays originally emitted in a direction further upstream, thus having a lower peak frequency. It is concluded that assuming a convection velocity independent on M_f allows a better match with experimental trends to be obtained than with the more classical expression of Eq. (3). The estimate from Ref. [21] gives also good predictions but in this model, the convection velocity first decreases with increasing flight speed and then increases, which is at odds with the other two models. An experimental survey would be needed to verify this evolution.

It has to be noted that Tam [13] obtains a much better absolute agreement while using Eq. (2) against the measurements of Norum & Shearin [12], with a convection velocity taken as in Eq. (3) with $\alpha = 0.7$. The discrepancy with the current results comes from the expression of shock spacing used by Tam, which is quite different from the one used here, but does not correspond to the present shock-cell measurements.

The effect of flight on the integrated sound pressure level (SPL) of BBSAN is displayed in Fig. 6 for constant θ_e . The SPLs have been obtained by simple integration of the spectra starting from the left of the broadband hump in order to exclude the low-frequency turbulent mixing noise. This technique assumes that the BBSAN dominates the turbulent mixing noise over the entire high frequency domain. Omitting the point at $M_f = 0.3$ which lies out of the trend defined by

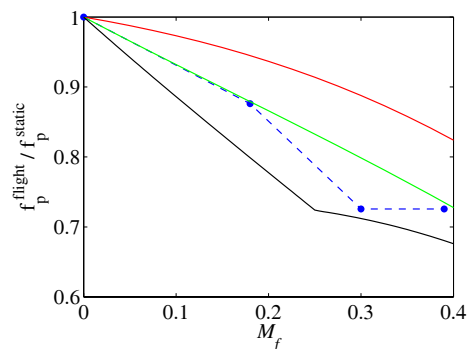


Figure 5: $f_p^{flight} / f_p^{static}$ for $M_j = 1.15$, $\theta_c = 99.5^\circ$.
 • measurement points, — U_c from Eq. (3), — U_c from Eq. (4), — U_c from Murakami & Papamoschou [21].

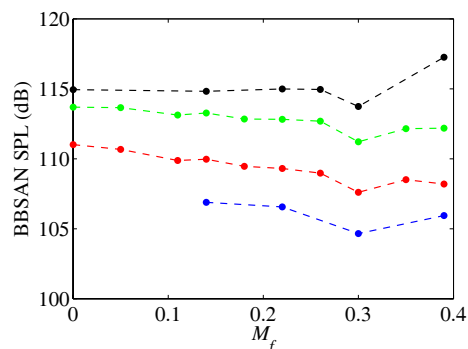


Figure 6: Integrated SPLs of BBSAN for $M_j = 1.15$.
 • $\theta_e = 37.5^\circ$, • $\theta_e = 80^\circ$, • $\theta_e = 100^\circ$, • $\theta_e = 130.5^\circ$.

the other points, a slight decrease of the SPL is noted for all angles but $\theta_e = 130.5^\circ$. This is in agreement with the results of Norum & Shearin [11]. For $\theta_e = 130.5^\circ$, the SPL seems rather to be independent on M_f . Other conclusions are reached when considering the peak amplitude of the broadband hump. Indeed, the peak value increases slightly with M_f , as if the shock-associated noise energy concentrated into the broadband hump. This is also similar to [11].

Now, preliminary PIV results are presented in order to explain the trends observed on the acoustical results.

4 PIV results

Three values of M_f have been investigated by PIV, namely $M_f = 0.05$, 0.22 and 0.39. The map of the norm of the mean velocity vectors is displayed in Fig. 7 for $M_f = 0.39$. The patch in the jet core from $x/D = 6$ to 10 conceals a region of the jet where condensation had darkened the PIV images and thus disrupted the velocity computation. This effect was however absent in the jet mixing layer.

It is known that broadband shock-associated noise arises from the interaction between the turbulence inside the jet mixing layer and the shock-cell system. As a consequence, both the shock-cell strength and the turbulence levels in the jet mixing layer have been estimated from the PIV results. The shock strength is defined here as the difference between the maximum mean velocity around the middle of each shock cell and the local minimum at the end of the same shock cell. The values of shock strength along the jet plume for all three values of M_f are displayed in Fig. 8 at $y = D_j/2$ (D_j is the

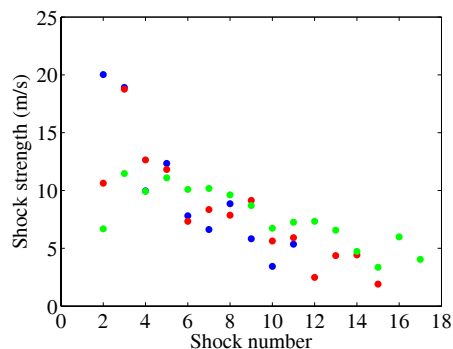


Figure 8: Shock strength computed from the mean velocity profile in the jet mixing layer at $M_j = 1.15$, $y = D_j/2$.
 • $M_f = 0.05$, • $M_f = 0.22$, • $M_f = 0.39$.

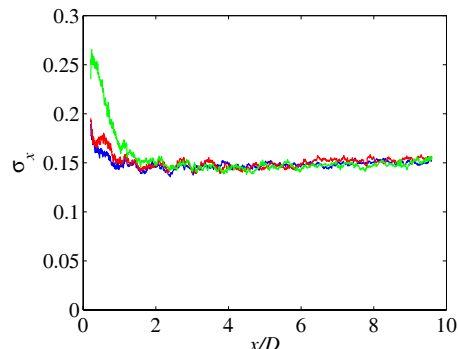


Figure 9: Longitudinal turbulence intensity level σ_x at $M_j = 1.15$, $y = D_j/2$. — $M_f = 0.05$, — $M_f = 0.22$, — $M_f = 0.39$.

fully expanded jet diameter). The shock-cell system extends further downstream with secondary flow but its strength does not seem to be affected by M_f . This is in agreement with Norum & Shearin's pressure measurements [12].

The evolution of a modified turbulence intensity based on the axial velocity, defined as $\sigma_x = v_x^{rms} / (U_j - U_f)$, is shown in Fig. 9. The three curves collapse, meaning that the turbulence level greatly decreases with increasing flight velocity. This arises from the reduced shear across the mixing layer. Associated with the practically unchanged shock strength in flight, this should lead to lower shock-associated noise levels. This is indeed the case when considering the integrated BBSAN sound pressure levels but the decrease was said to be quite small. Recalling that the BBSAN sources are thought to rather be the downstream shock cells than the upstream ones [19], the extension of the source region, coming from the flight-induced appearance of new shock cells further downstream, may be a balancing effect of the reduced turbulence levels, leading to the somewhat unchanged BBSAN levels. It is also possible that the mean turbulence intensity computed here is too global a parameter to conclude on the evolution of the part of the turbulence relevant for BBSAN generation. Hence, it could be of interest to investigate into the spectral components of turbulence.

5 Conclusion

An experimental study of flight effects on the broadband shock-associated noise component of an underexpanded su-

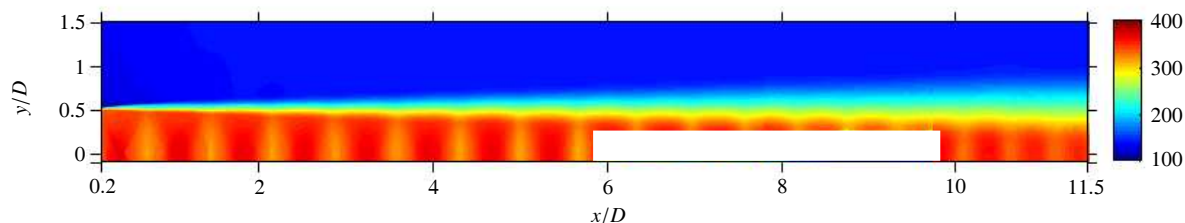


Figure 7: Map of the norm of the mean velocity vectors, $M_j = 1.15$, $M_f = 0.39$. The colorbar scale is in m/s.

personic jet has been performed using a free jet facility. Far-field acoustic measurements have been analysed to extract the peak frequency of the broadband hump and the sound pressure level of BBSAN. The measured frequencies have been compared to the prediction formula by Tam [13] with a set of estimates for the shock spacing and the convection velocity. It has been shown that a constant convection velocity with M_f led to a better agreement than the more usual expression displayed in Eq. (3). A slight decrease of the integrated BBSAN sound pressure level in flight has been identified. The PIV results show that the shock-cell strength seems practically independent on the flight velocity and that new shock cells appear in flight in the downstream part of the jet plume. On the other hand, the turbulence levels in the mixing layer decrease considerably between $M_f = 0.05$ and 0.39. It is possible that the source extension due to flight balances the reduced turbulence levels leading to the somewhat unchanged BBSAN levels.

Convection velocity measurements could permit to be assured of the expression to consider for frequency prediction. Phase averaging of the instantaneous velocity fields in screeching jets could lead to such an estimate.

Acknowledgments

The authors wish to thank Nathalie Grosjean for her help in setting up the PIV system. Thanks are also due to Airbus Operations SAS (Mauro Porta) and Snecma (Guillaume Bodard) for their joint financial support.

References

- [1] A. Powell, "On the Mechanism of Choked Jet Noise", *Proceedings of the Physical Society of London*, **66**, 1039-1056 (1953)
- [2] G. Raman, "Advances in understanding supersonic jet screech : Review and perspective", *Progress in Aerospace Sciences*, **34**, 45-106 (1998)
- [3] D. L. Martlew, "Noise associated with shock waves in supersonic jets", *AGARD CP*, **42**, 7-1 – 7-10 (1969)
- [4] M. Harper-Bourne, M. L. Fisher, "The noise from shock waves in supersonic jets", *AGARD CP*, **131**, 11-1 – 11-13 (1973)
- [5] H. K. Tanna, "An experimental study of jet noise Part II: Shock associated noise", *Journal of Sound and Vibration*, **50**, 429-444 (1977)
- [6] C. K. W. Tam, H. K. Tanna, "Shock associated noise of supersonic jets from convergent-divergent nozzles", *Journal of Sound and Vibration*, **81**, 337-358 (1982)
- [7] C. K. W. Tam, J. A. Jackson, J. M. Seiner, "A multiple-scales model of the shock-cell structure of imperfectly expanded supersonic jets", *Journal of Fluid Mechanics*, **153**, 123-149 (1985)
- [8] C. K. W. Tam, "Stochastic model theory of broadband shock-associated noise from supersonic jets", *Journal of Sound and Vibration*, **116**, 265-302 (1987)
- [9] W. D. Bryce, R. A. Pinker, "The noise from unheated supersonic jets in simulated flight", *AIAA Paper 77-1327* (1977)
- [10] T. D. Norum, J. G. Shearin, "Effects of simulated flight on the structure and noise of underexpanded jets", *NASA Technical Paper 2308* (1984)
- [11] T. D. Norum, J. G. Shearin, "Shock noise from supersonic jets in simulated flight to Mach 0.4", *AIAA Paper 86-1945* (1986)
- [12] T. D. Norum, J. G. Shearin, "Shock structure and noise of supersonic jets in simulated flight to Mach 0.4", *NASA Technical Paper 2785* (1988)
- [13] C. K. W. Tam, "Broadband shock-associated noise from supersonic jets in flight", *Journal of Sound and Vibration*, **151**, 131-147 (1991)
- [14] K. Viswanathan, M. J. Czech, "Measurement and modeling of effect of forward flight on jet noise", *AIAA Journal*, **49**, 216-234 (2011)
- [15] O. Rask, J. Kastner, E. Gutmark, "Understanding how chevrons modify noise in a supersonic jet with flight effects", *AIAA Journal*, **49**, 1569-1576 (2011)
- [16] B. André, T. Castelain, C. Bailly, "Experimental study of flight effects on screech in underexpanded jets", *Physics of Fluids*, **23**, 126102 (2011)
- [17] R. K. Amiet, "Refraction of sound by a shear layer", *Journal of Sound and Vibration*, **58**, 467-482 (1978)
- [18] B. André, T. Castelain, C. Bailly, "Broadband shock-associated noise in screeching and non-screeching underexpanded supersonic jets", *To appear in Ercoftac bulletin, Vol. 90*
- [19] T. D. Norum, J. M. Seiner, "Broadband shock noise from supersonic jets", *AIAA Journal*, **20**, 68-73 (1982)
- [20] P. J. Morris, "A note on the effect of forward flight on shock spacing in circular jets", *Journal of Sound and Vibration*, **121**, 175-177 (1988)
- [21] E. Murakami, D. Papamoschou, "Eddy convection in coaxial supersonic jets", *AIAA Journal*, **38**, 628-635 (2000)